

Christian Davidson
Xiangchun Xuan

Department of
Mechanical Engineering,
Clemson University,
Clemson, SC, USA

Received July 27, 2007
Revised September 7, 2007
Accepted September 8, 2007

Research Article

Effects of Stern layer conductance on electrokinetic energy conversion in nanofluidic channels

A thermo-electro-hydro-dynamic model is developed to analytically account for the effects of Stern layer conductance on electrokinetic energy conversion in nanofluidic channels. The optimum electrokinetic devices performance is dependent on a figure of merit, in which the Stern layer conductance appears as a nondimensional Dukhin number. Such surface conductance is found to significantly reduce the figure of merit and thus the efficiency and power output. This finding may explain why the recently measured electrokinetic devices performances are far below the theoretical predictions where the effects of Stern layer conductance have been ignored.

Keywords:

Dukhin number / Electrokinetic / Energy conversion / Figure of merit / Stern layer conductance
DOI 10.1002/elps.200700549



1 Introduction

Newfound attention has been given to electrokinetic energy conversion devices including electroosmotic pumps ([1–12], see ref. [7] for a review of micropumps by Laser and Santiago) and electrokinetic generators [13–17] due to their potential for integration into micro- and nanofluidic systems. Recent efforts have focused on increasing the efficiency of electrokinetic energy conversion in nanochannels, which, however, still seem much lower than that predicted by current theory [3, 9–17]. One likely explanation of this discrepancy is the neglect of Stern layer conductance in the electrokinetic theory [3, 9, 10, 14]. The Stern layer is the layer of counterions that attach to a charged surface. It is the inner immobile layer of the well-known electric double layer [18]. The electric conductance of the Stern layer has been found to significantly affect the electrokinetic transport of colloidal particles [19, 20]. Recently, van der Hayden *et al.* [14] included the contribution of this surface conductance in a chemical equilibrium model, which explained fairly well their measurements on a nanofluidic power generator. However, the real

effects of Stern layer conductance on electrokinetic devices performance (*e.g.*, efficiency and power output) are still largely unexplored. This article addresses this issue using an analytical thermo-electro-hydro-dynamic approach developed by Xuan and Li [21]. A similar approach was also used recently to analyze electrokinetic generating [13] and pumping efficiencies [12] in the absence of Stern layer conductance.

2 Theoretical formulation

2.1 Thermodynamic analysis

Electrokinetic energy conversion devices can be thermodynamically described by the Onsager reciprocal relations for volumetric flow rate, Q , and electric current, I , through a channel of arbitrary geometry [22, 23]

$$Q = G(-\Delta p) + M(-\Delta\phi) \quad (1)$$

$$I = M(-\Delta p) + S(-\Delta\phi) \quad (2)$$

where Δp and $\Delta\phi$ are the pressure difference and electric potential difference across the channel, G indicates the hydrodynamic conductance, M characterizes the EOF/

Correspondence: Professor Xiangchun Xuan, Department of Mechanical Engineering, Clemson University, Clemson, SC 29634-0921, USA
E-mail: xcxuan@clemson.edu
Fax: +1-864-656-7299

streaming current, and S denotes the electrical conductance. With these two phenomenological equations, Xuan and Li [21] have shown that the efficiency of electrokinetic energy conversion is independent of the working mode (*i.e.*, generator or pump) at the condition of maximum efficiency or maximum output power. Here, we present only the efficiency η and the output power W of an electrokinetic generator at the condition of maximum efficiency

$$\eta_{\max \eta} = \frac{z}{2(2-z)} \quad (3)$$

$$W_{\max \eta} = G \frac{\sqrt{1-Z}(1-\sqrt{1-Z})^2}{Z} (\Delta p)^2 \quad (4)$$

$$Z = \frac{M^2}{GS} \quad (5)$$

where Z is the previously termed “figure of merit” [21, 24, 25]. This nondimensional parameter, as shown below, is a function of fluid and channel properties.

2.2 Electro-hydro-dynamic analysis

Consider a slit nanochannel of height $2h$, width b , and length l where $b \gg 2h$ and $l \gg 2h$. One can then ignore the end effects and treat the channel as infinite parallel plates. In such a channel, the axial fluid velocity u of a combined pressure-driven and EOF is given by [26, 27]

$$u = \frac{h^2}{2\mu} \left(1 - \frac{y^2}{h^2}\right) \left(-\frac{\Delta p}{l}\right) + \frac{\varepsilon \zeta}{\mu} \left(\frac{\psi}{\zeta} - 1\right) \left(-\frac{\Delta \phi}{l}\right) \quad (6)$$

where μ is the fluid viscosity, y the transverse coordinate in the height direction that originates from the channel center, ε the fluid permittivity, ζ the zeta potential on the channel wall, and ψ is the electric double-layer potential.

To account for the Stern layer conductance, we propose the introduction of a new term into the traditional current density equation [26, 27], *i.e.*, the last term in Eq. (7)

$$i = -\varepsilon \frac{d^2 \psi}{dy^2} u + \sigma_b \cosh\left(\frac{z_v e \psi}{k_B T}\right) \left(\frac{-\Delta \phi}{l}\right) + \frac{\sigma_{\text{Stern}}}{h} \left(\frac{-\Delta \phi}{l}\right) \quad (7)$$

where σ_b is the bulk conductivity of the fluid, z_v the valence of ions, e the charge of proton, k_B the Boltzmann's constant, T the fluid temperature, and σ_{Stern} is the Stern layer conductivity. The Stern layer conductance term in Eq. (7) is derived from $(\sigma_{\text{Stern}} C/l)(-\Delta \phi)/A$ where, $C = 2(b + 2h)$ and $A = 2bh$ are the perimeter and the area of the channel cross-section, respectively. The other two terms in Eq. (7) indicate the streaming current density (first term) and the conduction current density (second term), respectively. Note that the

surface conductance of the diffuse layer has been considered in the conduction current density in terms of the $\cosh(x)$ function [26, 27]. This surface conductance should be distinguished from the Stern layer conductance.

Integrating Eqs. (6) and (7) over the channel cross-section and then comparing with Eqs. (1) and (2) yield the expressions of phenomenological coefficients (see Section 6 for the derivation)

$$G = \frac{2bh^3}{3\mu l} \quad (8)$$

$$M = -\frac{2bh\varepsilon\zeta}{\mu l} g_1 \quad (9)$$

$$S = \frac{4b\varepsilon^2 \zeta^2 K^2}{\mu h l \zeta^{*2}} \left[\left(1 + \frac{\beta}{4}\right) g_3 - \cosh(\Psi_0) + \frac{\beta}{4} Du \right] \quad (10)$$

$$g_1 = \int_0^h \left(1 - \frac{\Psi}{\zeta^*}\right) d\left(\frac{y}{h}\right) \quad (11)$$

$$g_3 = \int_0^h \cosh(\Psi) d\left(\frac{y}{h}\right) \quad (12)$$

Within these definitions, $\Psi = z_v e \psi / k_B T$ is the normalized double-layer potential where Ψ_0 the potential at the channel center; $\zeta^* = z_v e \zeta / k_B T$ the normalized zeta potential; $K = \kappa h$ the nondimensional channel height where $\kappa = \sqrt{2z_v^2 e^2 N_A c_b / \varepsilon k_B T}$ the inverse of Debye screening length, c_b the ionic concentration of the bulk fluid, and N_A is the Avogadro's number [18, 28]; $\beta = \Lambda \mu / \varepsilon R T$ is the nondimensional property of the working fluid where Λ is the molar conductivity and R is the universal gas constant (note: the reciprocal of β is previously termed the Levine number by Griffiths and Nilson [10]); and $Du = \sigma_{\text{Stern}} / h \sigma_b = \sigma_{\text{Stern}} / h \Lambda c_b$ is the Dukhin number. It is acknowledged that our Dukhin number is different from the traditional definition in which the numerator is the total surface conductance (*i.e.*, the conductance through both the inner Stern layer and outer diffuse layer) instead of the current Stern layer conductance [29, 30].

Combining Eqs. (8)–(10) with Eq. (5), we arrive at the figure of merit, Z , in the presence of Stern layer conductance effects

$$Z = \frac{3\zeta^{*2} g_1^2}{2K^2 \left[\left(1 + \frac{\beta}{4}\right) g_3 - \cosh(\Psi_0) + \frac{\beta}{4} Du \right]} \quad (13)$$

One can see that Z is a function of four nondimensional parameters, *i.e.*, β , K , ζ^* , and Du , as defined above. Apparently, the inclusion of Stern layer conductance decreases the figure of merit, Z , and hence reduces the efficiency of electrokinetic energy conversion, see Eq. (3). As will be seen shortly, Stern layer conductance also decreases the generation power in Eq.

(4) because the value of the figure of merit Z is reduced significantly.

The double-layer potential Ψ in the defined functions g_1 and g_3 are solved from the Poisson–Boltzmann equation [18]

$$\frac{d^2\Psi}{dy^2} = \kappa^2 \sinh(\Psi) \quad (14)$$

The analytical solution to Ψ is expressed in terms of the Jacobian elliptical function [31]

$$\Psi = \Psi_0 + 2 \ln \left[\text{JacCD} \left(\frac{\kappa y}{2} e^{-\Psi_0/2} \middle| e^{2\Psi_0} \right) \right] \quad (15)$$

where Ψ_0 is the double-layer potential at the channel center first defined in Eq. (10) and can be determined from the known zeta potential ζ (more precisely, ζ^*) on the channel wall. It is important to note that for a given fluid and channel combination, ζ will, in general, vary with the nondimensional channel height $K = \kappa h$. One option to address this is to use a surface-charge based potential parameter for scaling instead of zeta potential [13, 16, 17, 32]. In this work and other studies [3, 4, 9–12, 15, 21, 26, 27, 33, 34], the zeta potential is used directly, as it may be readily determined through experiment and provides a direct measure of the electroosmotic mobility.

3 Results and discussion

To examine quantitatively the effects of Stern layer conductance on electrokinetic devices performance, KCl aqueous solution with the concentration of $c_b = 10^{-5}$ M is used as the working fluid. Its properties include the viscosity $\mu = 0.9 \times 10^{-3} \text{ kg} \cdot \text{m}^{-1} \cdot \text{s}^{-1}$, dielectric constant $\varepsilon = 79 \times 8.854 \times 10^{-12} \text{ C} \cdot \text{V}^{-1} \cdot \text{m}^{-1}$, and molar conductivity $\Lambda = 0.0144 \text{ S} \cdot \text{m}^2 \cdot \text{mol}^{-1}$ at temperature $T = 298$ K [14]. The calculated Levine number is $\beta = 7.47$. The Stern layer conductance is assumed to be $\sigma_{\text{Stern}} = 1$ nS, as measured by Löbbus *et al.* [30] in a 1 mM KCl solution at pH 7.4. A MATLAB program (see the Supporting Information) was written to implement the calculations. An iterative method was first employed to determine the double-layer potential Ψ_0 from Eq. (15). Then, a direct numerical integration approach was applied to compute the phenomenological coefficients, figure of merit Z , and in turn the power output and efficiency of electrokinetic generators as an example.

Figure 1 displays the contour plots of the figure of merit Z (a) with and (b) without consideration of Stern layer conductance (*i.e.*, the Dukhin number, Du) over a range of $0 < K < 8$ and $0 < \zeta^* < 8$. As noted earlier, Stern layer conductance reduces Z significantly across the entire contour. Moreover, it is found that the region at which Z is maximized (and hence the generation efficiency $\eta_{\text{max}\eta}$ is maximized, see Eq. (3) and the discussion for Fig. 2) is more tightly focused in an area of high ζ^*/K values compared to that without

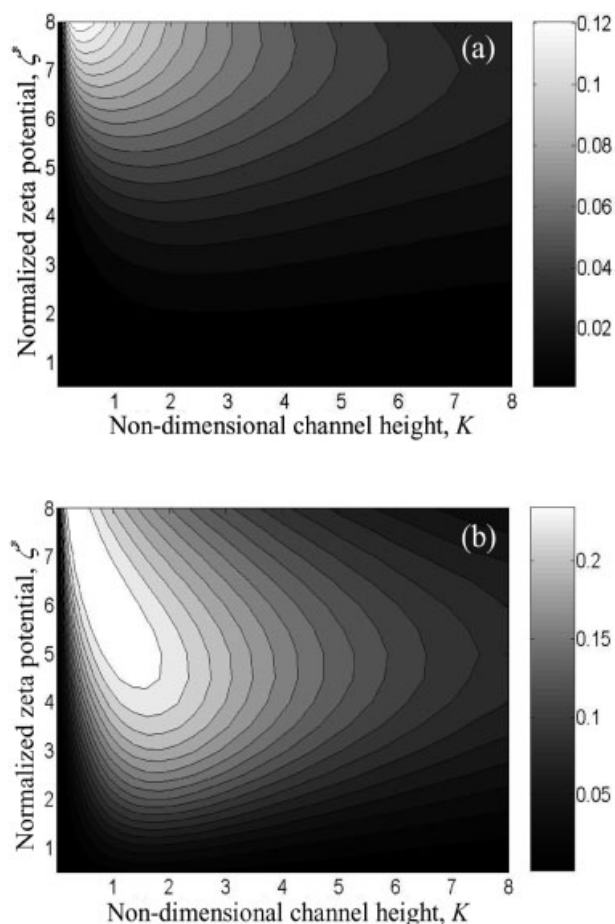


Figure 1. Contours of the figure of merit Z as a function of the normalized zeta potential ζ^* and the nondimensional channel height K when Stern layer conductance is (a) considered and (b) ignored.

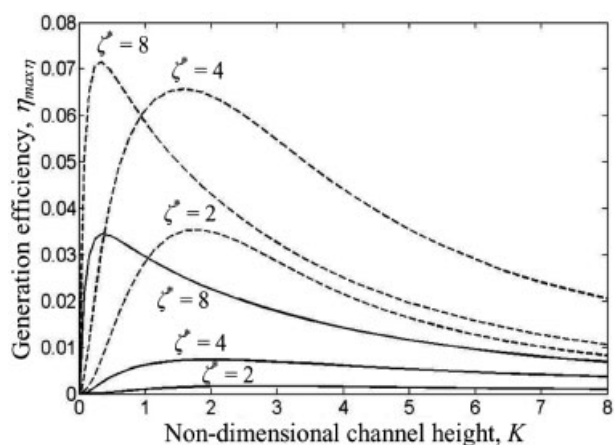


Figure 2. Comparison of the generation efficiency $\eta_{\text{max}\eta}$ when Stern layer conductance is considered (solid lines) and ignored (dashed lines). The highest efficiencies obtained, accounting for the Stern layer conductance, occur at $K = 0.34, 1.61,$ and 2.75 for $\zeta^* = 2, 4,$ and 8 , respectively.

accounting for the Stern layer conductance. With the assumed value of Stern layer conductance, *i.e.*, $\sigma_{\text{Stern}} = 1 \text{ nS}$, our results indicate that the optimum $Z = 0.12$ can only be obtained at about $\zeta^* = 8$ and $K = 0.5$. If $\sigma_{\text{Stern}} = 0$, however, a much higher value of $Z = 0.23$ can be achieved even at a zeta potential as low as $\zeta^* = 4.5$.

Figure 2 compares the maximum efficiency, *i.e.*, $\eta_{\text{max}\eta}$ in Eq. (3), of electrokinetic generators with (solid lines) and without (dashed lines) consideration of Stern layer conductance at $\zeta^* = 2, 4$, and 8 , respectively. As expected, $\eta_{\text{max}\eta}$ is diminished across the entire range of ζ^* and K values when the Stern layer conductance is accounted for. However, it is interesting and important to note that this conductance is more detrimental to the device efficiencies at lower zeta potentials. At $\zeta^* = 8$ the Stern layer conductance reduces the maximum obtainable efficiency, for any K value, by about 50% in comparison to nearly 95% at $\zeta^* = 2$. This phenomenon can be explained by examining the behavior of terms g_3 and $\cosh(\psi_0)$ in Eq. (13) which both increase exponentially as ζ^* rises. This causes Du to be less dominant for higher ζ^* values. In addition, it is noted that the value of K at which $\eta_{\text{max}\eta}$ is optimized stays almost constant at $\zeta^* = 8$ while increasing at $\zeta^* = 2$ and 4 by 33 and 47%, respectively, due to the effects of Stern layer conductance.

Figure 3 shows the contour plots of the normalized electrokinetic generation power density, *i.e.*, $W_{\text{max}\eta}$ in Eq. (4) normalized by the product of the channel volume, $V = 2bhl$, and the square of the applied pressure gradient, $P = \Delta p/l$

$$\frac{W_{\text{max}\eta}}{VP^2} = \frac{h^2 \sqrt{1-Z}(1-\sqrt{1-Z})^2}{3\mu Z} \quad (16)$$

when the Stern layer conductance is (a) considered and (b) ignored, respectively. Similar to the figure of merit and generation efficiency, Stern layer conductance also reduces the generation power across the entire contour. However, this conductance does not change the tendency of the generation power to scale with K (or the channel height h , see Eq. 16). Another notable effect of Stern layer conductance is that the optimum ζ^* value at which the generation power density is maximized has been shifted upwards from $\zeta^* = 5$ to about $\zeta^* = 7$. This change is inline with our other results as discussed above.

4 Concluding remarks

We have attempted to analytically determine the effects of Stern layer conductance in electrokinetic energy conversion devices. This conductance that has been neglected in previous studies appears in the total electric conductance in terms of Dukhin number. The new figure of merit Z thus becomes dependent on four nondimensional parameters: Levine number, normalized zeta potential ζ^* , nondimensional channel height K , and Dukhin number, Du . It is

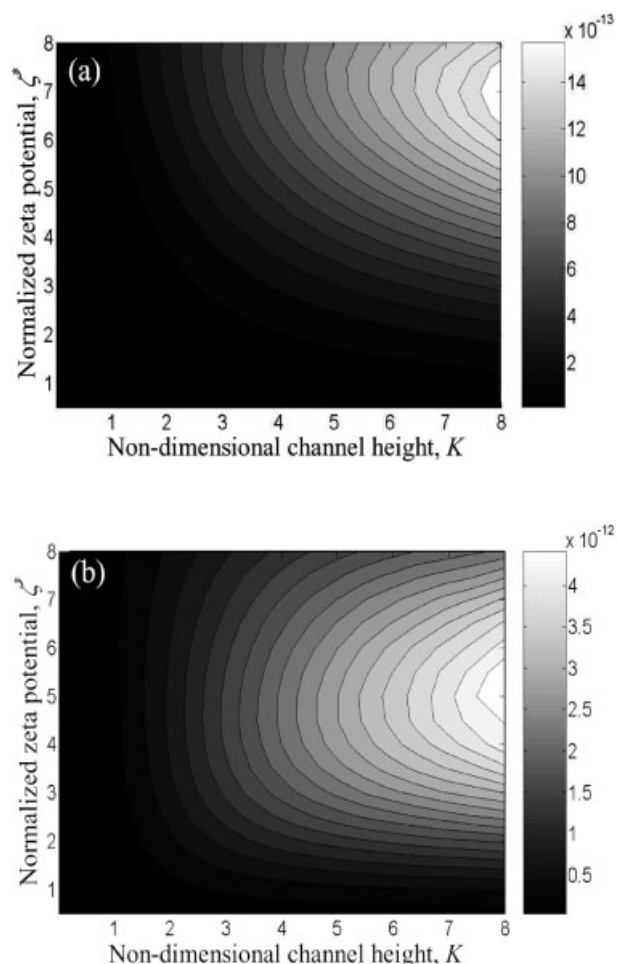


Figure 3. Contours of the normalized generation power density as a function of the normalized zeta potential, ζ^* and the non-dimensional channel height K when Stern layer conductance is (a) considered and (b) ignored.

found that Stern layer conductance reduces the efficiency and power output over the entire range of ζ^* and K values that are of practical interest due to the decrease in figure of merit. This phenomenon may explain why the recently measured electrokinetic device performances are far below previous theoretical predictions that ignored the contribution of Stern layer conductance. Our results also show that Stern layer conductance shifts the locations of optimal electrokinetic device performance toward the realm of higher ζ^* values.

Financial support from Clemson University through a start-up package to X. X. is gratefully acknowledged. The authors also thank Dr. Sven Holger Behrens and Dr. Frank van der Heyden for helpful discussions on the use of Eq. (15).

The authors have declared no conflict of interest.

5 References

- [1] Zeng, S., Chen, C., Mikkelsen, J. C., Santiago, J. G., *Sens. Actuators B* 2001, 79, 107–114.
- [2] Zeng, S., Chen, C., Mikkelsen, J. C., Santiago, J. G. *et al.*, *Sens. Actuators B* 2002, 82, 209–212.
- [3] Chen, C., Santiago, J. G., *J. Microelectromech. Syst.* 2002, 11, 672–683.
- [4] Yao, S., Santiago, J. G., *J. Colloid Interface Sci.* 2003, 268, 133–142.
- [5] Yao, S., Hertzog, D. E., Zeng, S., Mikkelsen, J. C., Santiago, J. G., *J. Colloid Interface Sci.* 2004, 268, 143–153.
- [6] Tripp, J. A., Svec, F., Fréchet, M. J., Zeng, S. *et al.*, *Sens. Actuators B* 2004, 99, 66–73.
- [7] Laser, D. J., Santiago, J. G., *J. Micromech. Microeng.* 2004, 14, R35–R64.
- [8] Reichmuth, D. S., Chirica, G. S., Kirby, B. J., *Sens. Actuators B* 2003, 92, 37–43.
- [9] Min, J. Y., Hasselbrink, E. F., Kim, S. J., *Sens. Actuators B* 2004, 98, 368–377.
- [10] Griffiths, S. K., Nilson, R. H., *Electrophoresis* 2005, 26, 351–361.
- [11] Min, J. Y., Kim, D., Kim, S. J., *Sens. Actuators B* 2006, 120, 305–312.
- [12] Chein, R. Y., Liao, J. C., *Electrophoresis* 2007, 28, 635–643.
- [13] van der Hayden, F. H. J., Bonthuis, D. J., Stein, D., Meyer, C., Dekker, C., *Nano Lett.* 2006, 6, 2232–2237.
- [14] van der Hayden, F. H. J., Bonthuis, D. J., Stein, D., Meyer, C., Dekker, C., *Nano Lett.* 2007, 7, 1022–1025.
- [15] Yang, J., Lu, F. Z., Kostyuk, L. W., Kwok, D. Y., *J. Micromech. Microeng.* 2003, 13, 963–970.
- [16] Daiguji, H., Yang, P., Szeri, A. J., Majumdar, A., *Nano Lett.* 2004, 4, 2315–2321.
- [17] Daiguji, H., Oka, Y., Adachi, T., Shirono, K., *Electrochem. Commun.* 2006, 8, 1796–1800.
- [18] Hunter, R. J., *Zeta Potential in Colloid Science: Principles and Applications*, Academic Press, New York 1981.
- [19] Mangelsdorf, C. S., White, L. R., *J. Chem. Soc. Faraday Trans.* 1990, 86, 2859–2870.
- [20] Rubio-Hernandez, F., Ruiz-Reina, E., Gomez-Merino, A. I., *Colloids Surf. A* 1999, 159, 373–379.
- [21] Xuan, X., Li, D., *J. Power Sources* 2006, 156, 677–684.
- [22] Brunet, E., Ajdari, A., *Phys. Rev. E* 2004, 69, 016306.
- [23] Brunet, E., Ajdari, A., *Phys. Rev. E* 2006, 73, 056306.
- [24] Morrison, F. A., Osterle, J. F., *J. Chem. Phys.* 1965, 43, 2111–2115.
- [25] Gross, R. J., Osterle, J. F., *J. Chem. Phys.* 1968, 49, 228–234.
- [26] Burgreen, D., Nakache, F. R., *J. Phys. Chem.* 1964, 68, 1084–1091.
- [27] Hildreth, D., *J. Phys. Chem.* 1970, 74, 2006–2015.
- [28] Li, D., *Electrokinetics in Microfluidics*, Elsevier Academic Press, Burlington, MA 2004.
- [29] Dukhin, S. S., Deryaguin, B. V., in: Matijevic, E. (Ed.), *Surface and Colloid Science*, Vol. 7, Wiley, London 1974.
- [30] Lbbus, M., Sonnfeld, J., Van Leeuwen, H. P., Vogelsberger, W., Lyklema, J., *J. Colloid Interface Sci.* 2000, 229, 174–183.
- [31] Behrens, S. H., Borkovec, M., *Phys. Rev. E* 1999, 60, 7040–7048.
- [32] De Leebeek, A., Sinton, D., *Electrophoresis* 2006, 27, 4999–5008.
- [33] Xuan, X., Li, D., *Electrophoresis* 2006, 27, 5020–5031.
- [34] Xuan, X., Li, D., *Electrophoresis* 2007, 28, 627–634.

6 Addendum

This Addendum provides a derivation for the phenomenological coefficient S in Eq. (10) in the main text. The derivations for the coefficients G and M are referred to Min *et al.* [9]. First integrate Eq. (7) over the cross-sectional area to determine the total electric current along the slit nanochannel of height $2h$ and width b

$$I = 2b \int_0^h -\varepsilon \frac{d^2\psi}{dy^2} u dy + 2b \int_0^h \sigma_b \cosh\left(\frac{z_v e \psi}{k_B T}\right) dy + 2b \int_0^h \frac{\sigma_{\text{Stern}}}{h} \left(\frac{-\Delta\phi}{l}\right) dy \quad (\text{A1})$$

Expanding the fluid velocity in the first term using Eq. (6) and grouping all terms give

$$I = \left[-\frac{bh^2\varepsilon}{\mu l} \int_0^h \frac{d^2\psi}{dy^2} \left(1 - \frac{y^2}{h^2}\right) dy \right] (-\Delta p) + \left[\frac{2b\varepsilon^2\zeta}{\mu l} \int_0^h \frac{d^2\psi}{dy^2} \left(1 - \frac{\psi}{\zeta}\right) dy + \frac{2b\sigma_b}{l} \int_0^h \cosh\left(\frac{z_v e \psi}{k_B T}\right) dy + \frac{2b\sigma_{\text{Stern}}}{l} \right] (-\Delta\phi) \quad (\text{A2})$$

Comparing Eq. (A2) with the phenomenological equation for electric current, *i.e.*, Eq. (2), immediately yields

$$S = \frac{2b\varepsilon^2\zeta^2}{\mu l\zeta^*} \int_0^h \left(\frac{d\Psi}{dy}\right)^2 \left(1 - \frac{\Psi}{\zeta^*}\right) dy + \frac{2b\sigma_b}{l} \int_0^h \cosh(\Psi) dy + \frac{2b\sigma_{\text{Stern}}}{l} \quad (\text{A3})$$

where $\Psi = z_v e \psi / k_B T$ and $\zeta^* = z_v \zeta e / k_B T$ are as defined in the main text. Applying integration by parts to the first term in Eq. (A3) receives

$$S = \frac{2b\varepsilon^2\zeta^2}{\mu l\zeta^{*2}} \int_0^h \left(\frac{d\Psi}{dy}\right)^2 dy + \frac{2b\sigma_b}{l} \int_0^h \cosh(\Psi) dy + \frac{2b\sigma_{\text{Stern}}}{l} \quad (\text{A4})$$

To further simplify the first term in Eq. (A4), we rewrite the Poisson-Boltzmann equation, Eq. (14), as follows

$$2 \frac{d\Psi}{dy} \frac{d^2\Psi}{dy^2} = 2\kappa^2 \sinh(\Psi) \frac{d\Psi}{dy} \quad (\text{A5})$$

which can then be rearranged as

$$d \left[\left(\frac{d\Psi}{dy}\right)^2 \right] = 2\kappa^2 \sinh(\Psi) d\Psi \quad (\text{A6})$$

Integrating Eq. (A6) with respect to Ψ leads to

$$\left(\frac{d\Psi}{dy}\right)^2 = 2\kappa^2[\cosh(\Psi) - \cosh(\Psi_0)] \quad (\text{A7})$$

where Ψ_0 is the normalized double-layer potential at the channel center. By defining the function g_3 , Eq. (12) in the main text, one can now specify the coefficient S in Eq. (A4) as

$$S = \frac{4b\epsilon^2\zeta^2 K^2}{\mu h \zeta^{*2}} [g_3 - \cosh(\Psi_0)] + \frac{2bh\sigma_b g_3}{l} + \frac{2b\sigma_{\text{Stern}}}{l} \quad (\text{A8})$$

Invoking $K = h$, $\kappa = \sqrt{2z_v^2 e^2 N_A c_b / \epsilon k_B T}$, $\sigma_b = \Lambda c_b$, $\zeta^* = z_v e \zeta / k_B T$, and $R = k_B N_A$ reduces Eq. (A8) to

$$S = \frac{4b\epsilon^2\zeta^2 K^2}{\mu h \zeta^{*2}} \left[g_3 - \cosh(\Psi_0) + \frac{\Lambda\mu}{4\epsilon RT} g_3 + \frac{\Lambda\mu}{4\epsilon RT} \frac{\sigma_{\text{Stern}}}{\sigma_b h} \right] \quad (\text{A9})$$

which is equivalent to Eq. (10) if one defines the Levine number $\beta = \Lambda\mu/\epsilon RT$ and the Dukhin number, $Du = \sigma_{\text{Stern}}/h\sigma_b$.